Online supplement of Beckers et al

Materials & Methods

RhoA activation In vivo

The investigation conforms with the *Guide for the Care and Use of Laboratory Animals* published by the US National Institutes of Health (NIH Publication No. 85-23, revised 1996) and was undertaken with approval of the local ethics committee. Male Wistar rats (n=6, 300-360g; Harlan, Horst, the Netherlands) were anesthetized with pentobarbital (i.p. 60 mg/kg) and ketamine HCl (i.m. 70 mg/kg) followed by a pentobarbital maintenance dose (i.p. 30 min/15 mg/kg). Rats were placed in a supine position on a heating pad maintaining body temperature at 37ºC. An intraperitoneal (i.p.) catheter was placed to administer pentobarbital. The trachea was intubated with polyethylene tubing to facilitate breathing. The animals received 75 IU/kg heparin (Leo Pharmaceutical Products, Weesp, the Netherlands) intravenously to prevent catheter clotting. Mean arterial pressure (100-120 mm Hg) and heart rate (340-380 beats per minute) were continuously monitored via a catheter in the carotid artery connected to a pressure transducer. Both femurs were uncovered by opening the skin and the femoral veins cannulated in in the direction of blood flow. Thrombin receptor activating peptide (TRAP) (Bachem, Germany) was infused at a dose of 1 mg/kg according to Chintala et al.(1) over a period of 5 minutes followed by formaldehyde (5 minutes) or saline and formaldehyde (15 minutes). The control received a sham procedure with saline instead of TRAP. Following TRAP exposure, 4% formaldehyde (Sigma) in saline was infused during 10 minutes for fixation of the veins. Thereafter, one minute infusion of 0.05% Triton X-100 (Sigma) in saline was used for permeabilization of the endothelial cells followed by a 5 minute washout with saline. Femoral veins were dissected, cut open longitudinally and fixed on silicone plates. Veins were incubated overnight with PBS containing 1% HSA, stained for RhoA-GTPase (Cytoskeleton, Denver, CO, USA) and F-actin with Rhodamine-Phalloidin 1:100 (Molecular Probes). After staining, veins were placed on a

microscope glass covered with hard mount Vectashield™ containing the nuclear stain DAPI (Vector Laboraties, Burlingame, CA, USA) and sealed using a cover slip.

Cell Culture

Umbilical cords were obtained from the Department of Obstetrics of the Amstelland Hospital in Amstelveen, The Netherlands. The investigation conforms to the principles outlined in the Declaration of Helsinki and was undertaken with approval of the local ethics committee. Human umbilical vein endothelial cells (HUVECs) were isolated from healthy donors as previously described with some minor modifications.(2) Cells were resuspended in Earl's balanced M199 supplemented with 2 mmol/l L-glutamine, 100 U/ml penicillin, 100 mg/ml streptomycin (all Biowhittaker, Verviers, Belgium), 10% heat-inactivated human serum (Sanquin CLB, Amsterdam, The Netherlands), 10% heat-inactivated new born calf serum (Gibco, Grand Island, NY), 5 U/ml heparin (Leo Pharmaceutical products, Weesp, The Netherlands) and 150 μg/ml crude endothelial cell growth factor prepared from bovine brains(3) and seeded in 1% gelatin coated plates (Costar, Cambridge, MA). Cells were cultured in 5% CO_2 at 37ºC. Confluent cells were washed with HBSS (Cambrex, Verviers, Belgium), trypsinized (0.05% trypsin, Gibco, Grand Island, NY) and seeded to 1/3 of their density. Cells were extensively characterized as endothelial cells.(4)

Raichu probes

Ras and interacting protein chimeric unit (Raichu) probes were a kind gift of Prof. M. Matsuda, Osaka University, Japan. Raichu-RhoA/RhoA-CT, which is hereafter called Raichu-RhoA, contains a Rho binding domain (RBD) and truncated RhoA (aa 1-189) between the two fluorophores and can thus be used to monitor the balance between rhoGEF and rhoGAP activities. Raichu-RBD-X, which lacks the functional RhoA-GTPase fragment, is useful for visualization of endogenous RhoA activation. Both of these probes contain the authentic CAAX-box of RhoA which is fused to the CFP

protein and enables the probes to localize with the endogenous RhoA. Raichu-RhoA/KRas-CT is essentially the same construct as Raichu-RhoA, but due to the carboxy terminal region of K-Ras4B, the probe localizes to the plasma membrane.

As evidenced by 3D-fluorescence-microscopy in fixed cells, the Raichu-RhoA biosensor localizes at junctional areas of confluent monolayers and is distributed rather homogenously throughout the cell, with some accumulation around the nucleus, at F-actin filaments, and at thrombin-induced F-actin stress fibers (suppl figure I). Note that during the study, except for movie 1, post-confluent ECs were used. This is not always obvious from the images, as transfection efficiency is in the lower 50% range. Moreover, transfection of ECs with the Raichu-RhoA biosensor did not affect baseline or thrombin-induced changes in endothelial barrier function as evidenced by ECIS measurements (data not shown). Thus, the Raichu-RhoA biosensor allowed for imaging of RhoA activity in relevant areas but did not hamper essential signaling events involved in the regulation of endothelial barrier function.

Endothelial Cell Transfection

Delta T Dishes (Biotechs Inc, Butler, USA) were coated with 1% gelatin and cross-linked with 0.5% glutaraldehyde (Fluka, St.Gallen, Switzerland). Dishes were washed 3 times with M199 and incubated overnight with 5 μg/ml fibronectin (Roche, Woerden, the Netherlands). HUVECs were transfected using Amaxa nucleofection according to the manufacturer's protocol (www.amaxa.com). In short, approximately 1 million cells with a confluence of about 90% were collected. 100 μl nucleofector solution (Amaxa, Cologne, Germany) and 4 μg of one of the Raichu-probes(5) was added. After electroporation, culture medium was added and cells were seeded to confluency in Delta T Dishes. Four hours after transfection the medium was replaced.

Experimental Conditions

Raichu-transfected HUVECs were cultured 2 to 3 days post-confluent.. At this stage, transfection efficiency was in the lower 50% range. For imaging, cells were chosen with moderate biosensor expression. Occasionally, cells were pre-incubated for 15 minutes with 2 μg/ml live cell Hoechst (Molecular Probes, Eugene, Oregon) after which the cells were washed and incubated with 1% HSA in Hank's balanced M199 (Biowhittaker, Verviers, Belgium) for 60 minutes. RhoA was inhibited by 2 hours pre-incubation of the cells with 1 μg/ml cell-permeable C3-transferase (Cytoskeleton, Denver, USA). During live cell imaging, cells were stimulated with 1 U/ml thrombin (Sigma, Missouri, USA) for 15 minutes, or 25 ng/ml VEGF for the indicated time periods, after which cells were fixated for 3D imaging.

3D Digital Imaging Microscopy

Cells for 3D imaging were fixed with 2% formaldehyde (Merck, Darmstadt, Germany) for 15 minutes on ice, permeabilized with 0.05% triton-x-100 (C2206, Sigma, Missouri, USA) for 1 minute, and washed twice with PBS. Cells were stained o/n for cortactin, and incubated with rhodamine-phalloidine (Molecular Probes, Eugene, Oregon) to stain for F-actin filaments for 30 minutes. Cells were washed and sealed in vectashield (Vector Laboratories, Peterborough, UK).

Imaging was performed with a Zeiss Axiovert 200 Marianas™ inverted microscope as described previously.(6) Briefly, a cooled Sensicam CCD camera (Cooke, Tonawanda, NY) combined with a motorized xy-stage and 40 and 63 x oil immersion Zeiss objective lenses under the control of Slidebook software (Intelligent Imaging Innovations, Denver, CO) allowed us to obtain 3D digital images after which constrained iterative deconvolution was performed.

Fluorescent Resonance Energy Transfer (FRET) microscopy

Three channel FRET microscopy was performed using the microscope described above, with a cyan/topaz energy transfer filter set (#31052) in combination with cyan and yellow fluorescent protein filters (#31044v2 and #41028, respectively; Chroma Technology Corporation, Rockingham, USA). Spectral bleed-through (SBT) was measured after transfection of HUVECs with either pEYFP (kind gift of Dr. J.A. Rodriguez, CCA, Amsterdam) or pECFP (kind gift of Dr. R. Bernad, NKI, Amsterdam). The donor (Fd/Dd) SBT and the acceptor (Fa/Aa) SBT for our setup are 0.349668 and 0.0221681, respectively. Chromatic aberration was checked using fluorescent microspheres (Molecular Probes, Eugene, Oregon).

RhoA activity was followed in time for 15 minutes. The interval time was 30 seconds. To minimize phototoxicity, the binning of the CCD camera was set to 2x2. Typical exposure time for the three channels together did not exceed 5 seconds. After the first 5 to 8 intervals (indicated per experiment), cells were stimulated with 1 U/ml thrombin (Sigma, Missouri, USA).

Three channel corrected FRET (FRETc) analyses was calculated, normalized for the acceptor concentration (FRETc/A), and presented using a pseudocolor map. Briefly, CFP is the donor channel, YFP the acceptor channel, and FRET the transfer channel. After background subtraction, FRETc was calculated by the following equation: FRET – (Fd/Dd * CFP) – (Fa/Aa * YFP), in which the donor spectral bleed - through (Fd/Dd * CFP) and the acceptor spectral bleed-through (Fa/Aa * YFP) are subtracted from the FRET signal. In this equation, each symbol starts with an uppercase letter representing the filter set, *D* for the Donor filter set and *F* for the FRET filter set. The second letter, in lowercase, indicates which fluorochromes are present in the specimen: *d* for donor only, *a* for acceptor only, and *f* for both donor and acceptor present (so FRET is possible).(7) Thus, *Fd* stands for the signal from a donor-only specimen using the FRET filter set, whereas *Dd* represents the signal from a donor-only specimen using the donor filter cube. *Fa* is the signal from an

acceptor-only specimen using the FRET filter set and *Aa* the signal from an acceptor-only specimen using the Acceptor filter.

Bearing in mind that three-channel FRET analysis is a user-dependent semi-quantitative method, our FRET data were analyzed by several investigators. To further ensure that the increase in FRETc/A intensity indeed reflected the activation of RhoA, cells were incubated with C3-transferase, a cell-permeable RhoA inhibitor, which blocked thrombin-mediated RhoA activation.

FRET analysis

For quantitative analysis of RhoA activity, the quantification function of the Slidebook software was used. After FRETc/A was obtained, where possible 5 to 10 regions were selected for FRETc/A intensity measurements, either at the cell margins or in the cell body. Intensity measurements were corrected for the background and presented as RhoA activity per region (FRETc/A intensity).

Furthermore, the 3D function of the Slidebook software was used to visualise the localization and intensity of RhoA activity, where the z-axis represents the intensity of RhoA activity.

Fluorescence resonance energy transfer (FRET) analysis by photobleach method.

FRET analysis by photobleach method in fixed cells was performed as previously described.(8) In short, rat-lung microvascular endothelial cells were transfected with Raichu-RhoA using Amaxa technology, grown on glass coverslips for 48 hrs, and fixed with 2% paraformaldehyde in PBS with 0.12 M sucrose. The fixed cells were viewed with a Zeiss LSM-510 META confocal imaging system equipped with a 50 mW argon laser and 25x objective. Cells that expressed CFP or YFP alone were imaged with a Zeiss META spectral detector. An image stack was generated with the 458 nm laser line spanning an emission wavelength range from 462.9 to 602 nm with bandwidths of 10.7 nm (pinhole of 1.66 Airy units and a vertical [*Z*] resolution of <2.0

μm). These spectra served as CFP and YFP reference emission signatures which were used in a linear unmixing algorithm (Zeiss AIM software) to separate the fluorescence contribution of CFP and YFP (on a pixel by pixel basis). Prebleach CFP and YFP images were collected using the argon laser with a 458 nm/514 nm dual dichroic. A selected region of interest (ROI) on the plasma membrane or in the cell body was irradiated with the 514 nm laser line (100% intensity) for 55 s (200 iterations) to photobleach YFP. Postbleach images were captured immediately. FRET in the ROI was evidenced by an increase in CFP fluorescence intensity (donor dequenching) following YFP (acceptor) photobleaching divided by CFP (post-bleach) according to the equation: [CFP(post-bleach) - CFP(pre-bleach) / CFP(post-bleach)]. The major advantage of using the photobleach method combined with the linear unmixing algorithm is that the potential pitfall of bleed-through artifact can be avoided.

Impedance time course

Cultureware, measurement equipment (ECIS 1600R), and software for data acquisition and analysis were obtained from Applied BioPhysics (Troy, NY). Standard ECIS culture plates (8W1E) were used. Each of the eight wells comprise a culture area of 0.8 cm^2 and contain a single circular gold-electrode (250 μm in diameter) and a much larger counter electrode. The electrodes were stabilized with L-cysteine (10 mM) before HUVEC were plated on the gelatin (1%) coated wells. Cells were allowed to form a monolayer for 72 hrs. Impedance values were obtained by applying a constant 4 kHz current flow (μA) through the endothelial layer and simultaneous measurement of resulting sum-potential were recorded. Resistance and capacitance calculationswere performed by the ECIS equipment. Impedance was recorded in the presence or absence of the indicated inhibitors.

Micromotion

It has been shown that small fluctuations in the impedance signal are due to cell movements on and off the electrode even in a confluent layer.(9) The analysis of this cell-mediated noise (micromotion) was performed on the basis of frequency analyses as described by Opp et al.(10). Data processing software was developed in our laboratory and written in LabVIEW (National Instruments, Austin). Resistance data were recorded every second for one hour at 4 kHz. The data set was broken into segments with a length of 256 data points. Each segment was multiplied by a Hanning window and run through a 256 point Fourier transformation. The resulting frequency spectra were averaged to a single-sided 129 point power spectrum, Thereby, random noise was minimized and the biological noise was elucidated. Frequency was plotted against amplitude in a log-log graph and a least squares linear fit was applied. The slope of the linear fit was used as a measure of overall noise and thereby micromotion.

Statistics

All data represented were confirmed in at least three experiments, unless otherwise noted. For basic statistical analysis SPSS software was used. Data were compared by a Student's *t*-test. *P*-values of less than 0.05 were considered to be significant.

Reference List

1. Chintala MS, Chiu PJ, Bernadino V, Tetzloff GG, Tedesco R, Sabin C, et al. Disparate effects of thrombin receptor activating peptide on platelets and peripheral vasculature in rats. Eur J Pharmacol 1998;349:237-43.

2. van Nieuw Amerongen GP, Koolwijk P, Versteilen A, van Hinsbergh VW. Involvement of RhoA/Rho kinase signaling in VEGF-induced endothelial cell migration and angiogenesis in vitro. Arterioscler Thromb Vasc Biol 2003;23:211-7.

3. Maciag T, Cerundolo J, Ilsley S, Kelley PR, Forand R. An endothelial cell growth factor from bovine hypothalamus: identification and partial characterization. Proc Natl Acad Sci U S A 1979;76:5674-8.

4. van Hinsbergh VWM, Draijer R. In vitro models and functional studies of endothelia. Culture, characterization and application of human endothelial cells. In: A.J.Shaw, ed. Cell culture models of epithelial tissues. A practical approach.: Oxford University Press, 1996:87-110.

5. Yoshizaki H, Ohba Y, Kurokawa K, Itoh RE, Nakamura T, Mochizuki N, et al. Activity of Rho-family GTPases during cell division as visualized with FRET-based probes. J Cell Biol 2003;162:223-32.

6. van der Sar AM, Musters RJ, van Eeden FJ, Appelmelk BJ, Vandenbroucke-Grauls CM, Bitter W. Zebrafish embryos as a model host for the real time analysis of Salmonella typhimurium infections. Cell Microbiol 2003;5:601-11.

7. Gordon GW, Berry G, Liang XH, Levine B, Herman B. Quantitative fluorescence resonance energy transfer measurements using fluorescence microscopy. Biophys J 1998;74:2702-13.

8. Chen Z, Deddish PA, Minshall RD, Becker RP, Erdos EG, Tan F. Human ACE and bradykinin B2 receptors form a complex at the plasma membrane. FASEB J 2006;20:2261-70.

9. Giaever I, Keese CR. Micromotion of mammalian cells measured electrically. Proc Natl Acad Sci U S A 1991;88:7896-900.

10. Opp D, Wafula B, Lim J, Huang E, Lo JC, Lo CM. Use of electric cell-substrate impedance sensing to assess in vitro cytotoxicity. Biosens Bioelectron 2009;24:2625-9.

Legends belonging to the Online supplement of Beckers et al.

Supplemental Figure I: Raichu-RhoA localization in fixed HUVECs.

Raichu-RhoA transfected HUVECs grown on Delta T dishes were fixed and counterstained for F-actin (red) and the nuclei (blue). Control cells in the left panel, thrombin-activated cells in the right panel (20 minutes after thrombin stimulation). For acquisition of the Raichu-RhoA signal, the YFP-channel was used. The arrows indicate Raichu-RhoA (green) at the cell margins of thrombin-stimulated ECs. Enlargement of boxes after deconvolution shows co-localization of Raichu-RhoA with the F-actin SFs (1,3) and with the thinner and more complex F-actin network in the cytoplasm (2,4).

Raichu-RhoA (green) is distributed rather homogenously throughout the cell, with some accumulation around the nucleus (blue) and at the cell margins (arrows). Deconvolution and enlargement of specific areas (white boxes in Fig. 1) revealed various co-localizations of Raichu-RhoA and the actin cytoskeleton (red). Box 1 and 3 show co-localization of Raichu-RhoA with the stress fibers, while box 2 and 4 show that Raichu-RhoA also co-localized with the thinner and more complex actin network in the cytoplasm.

Supplemental figure II: Thrombin-enhanced RhoA activity at the cell margins.

Quantitative analysis of RhoA activity using a linear unmixing algorithm in rat lung microvascular ECs as described in the Methods section.

A: A representative example of prebleach and postbleach CFP and YFP images. A selected region of interest (ROI) on the plasma membrane was photobleached in fixed cells. Postbleach images were captured immediately afterwards. FRET in the ROI was evidenced by an increase in CFP fluorescence intensity (donor dequenching) following YFP (acceptor) photobleaching.

B: Quantitative analysis of the time-course of thrombin-enhanced RhoA activation.

C: Thrombin enhances the mean RhoA activity at the cell periphery, but not in the cytoplasm. Quantitative analysis of RhoA activity in membrane and cytoplasmic areas using a linear unmixing algorithm in fixed rat lung microvascular ECs as described in the online Methods section. Data are mean ± SD of at least 6 determinations.

Supplemental figure I II: Thrombin-induced RhoA acti vity at F-a ctin stress fibers.

Raichu-RhoA transfected HUVECs were grown on Delta T dishes. During time-lapse imaging with an interval time of 30 seconds the cells were stimulated with thrombin at t=2 min.

A: The left panel shows the localization of Raichu-RhoA by YFP acquisition and the right panel shows RhoA activity displayed as a pseudo-color thermal map corresponding to the scale shown in the right upper corner. The arrow indicates a continuously contracting fiber in the upper cell after thrombin stimulation. Region 2 was set around this fiber.

B: Quantification of RhoA activity in region 2 (graph, orange line) shows continuously high RhoA activity after thrombin stimulation. Region 1 (purple line) was set around the membrane and shows a rapid increase and decrease of RhoA activity upon thrombin stimulation.

C: *Raichu-Rho probe at finger-like bridges prior to separation of ECs.*

Raichu-RhoA transfected HUVECs were grown on Delta T dishes. During time-lapse imaging with an interval time of 30 seconds the cells were stimulated with thrombin at t=2½ min. A) Thrombin stimulated Raichu-RhoA transfected cells were fixed and stained for F-actin (red). For acquisition of Raichu-RhoA (green) the YFP-channel was used. The upper panel shows the raw images, the middle panel the deconvolved

images. The box contains a finger-like bridge between the separating cells, which is enlarged in the lower panel.

Supplemental figure IV. Inhibition of Rho kinase leads to decreased protrusive membrane activity. DIC image stacks were taken with a distance of 0.28 µm in the z-direction between every image and a 40-times magnification. For better visualization, the presented pictures are further enlarged by a zoom factor of four.

A1-3) Finger-like protrusions (arrows) are present in confluent endothelial monolayers under basal conditions. These three dimensional structures are exclusively located at the cell membrane.

A4) The merged pixel cross section of all 25 stacks shows, how highly active the protrusions are.

B1-3) Hardly any membrane protrusion is visible after incubation with Y-27632 (1 µM) for 24 hrs.

Supplemental Figure V: VEGF-induced inter-endothelial gap formation is not preceded by local RhoA activation. Time-lapse imaging of Raichu-RhoA transfected HUVECs grown on Delta T dishes. ECs were stimulated with VEGF (25 ng/ml) at t=2.5 min.

Movie 1. RhoA activity at the membrane ruffles of non-stimulated, sub-confluent HUVECs.

Raichu-RhoA transfected HUVECs were grown on Delta T dishes. During time-lapse imaging with an interval time of 30 seconds the localization of Raichu-RhoA as well as the activation of RhoA was obtained. The three channel corrected FRET analysis was normalised for the acceptor concentration as described in Materials & Methods. RhoA activity is displayed as a pseudo-colour thermal map corresponding to the

scale shown in the right upper corner. Red corresponds to high RhoA activity and blue to low RhoA activity. Note the increased RhoA activity at the membrane ruffles and the absence of RhoA activation where the adjacent cells are connected.

Movie 2. Thrombin enhanced RhoA activity at the cell margins of confluent HUVECs.

Raichu-RhoA transfected HUVECs were grown on Delta T dishes. During time-lapse imaging with an interval time of 30 seconds the cells were stimulated with thrombin at t=3 min. Three channel corrected FRET analysis was normalized for the acceptor concentration as described in Materials & Methods. RhoA activity is displayed as a pseudo-colour thermal map corresponding to the scale shown in the right upper corner. Red corresponds to high RhoA activity and blue to low RhoA activity.

Movie 3. Low RhoA activity at the cell margins of non-stimulated, confluent HUVECs.

Raichu-RhoA transfected HUVECs were grown on Delta T dishes. During time-lapse imaging with an interval time of 30 seconds the cells were stimulated with thrombin at t=3 min. Three channel corrected FRET analysis was normalized for the acceptor concentration as described in Materials & Methods. RhoA activity is displayed as a pseudo-colour thermal map corresponding to the scale shown in the right upper corner. Red corresponds to high RhoA activity and blue to low RhoA activity.

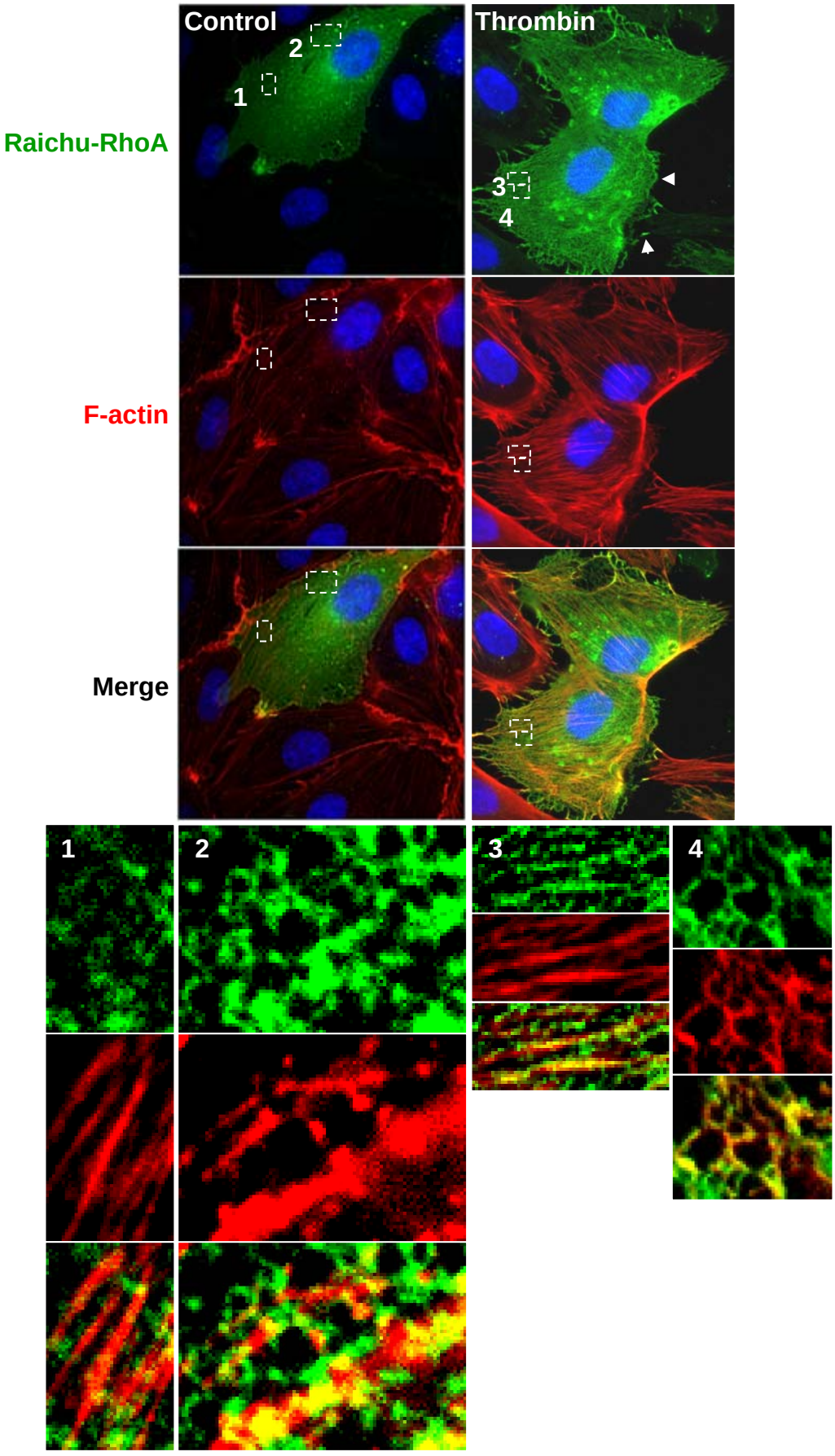

Suppl Figure I

A

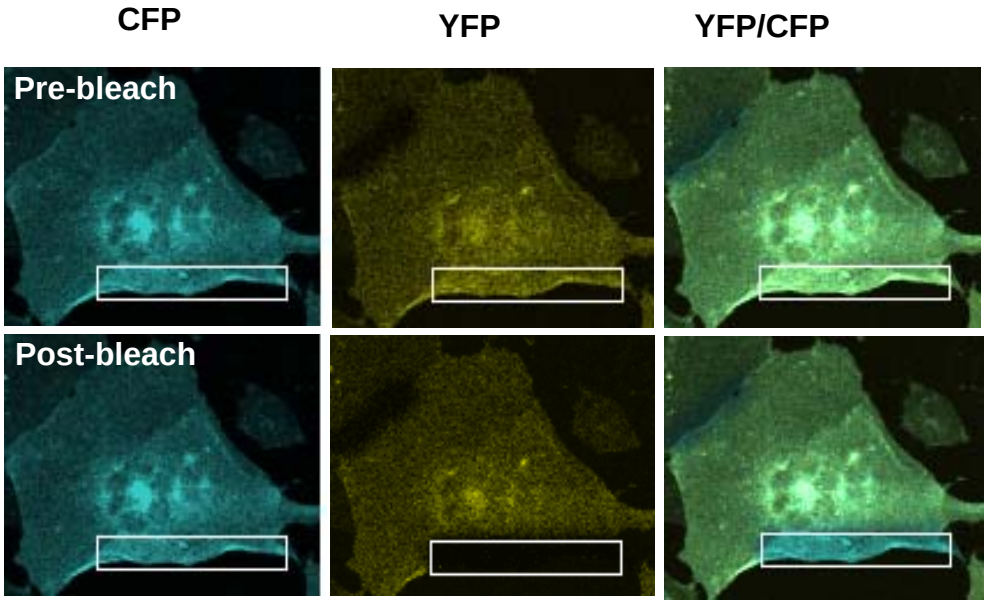

B

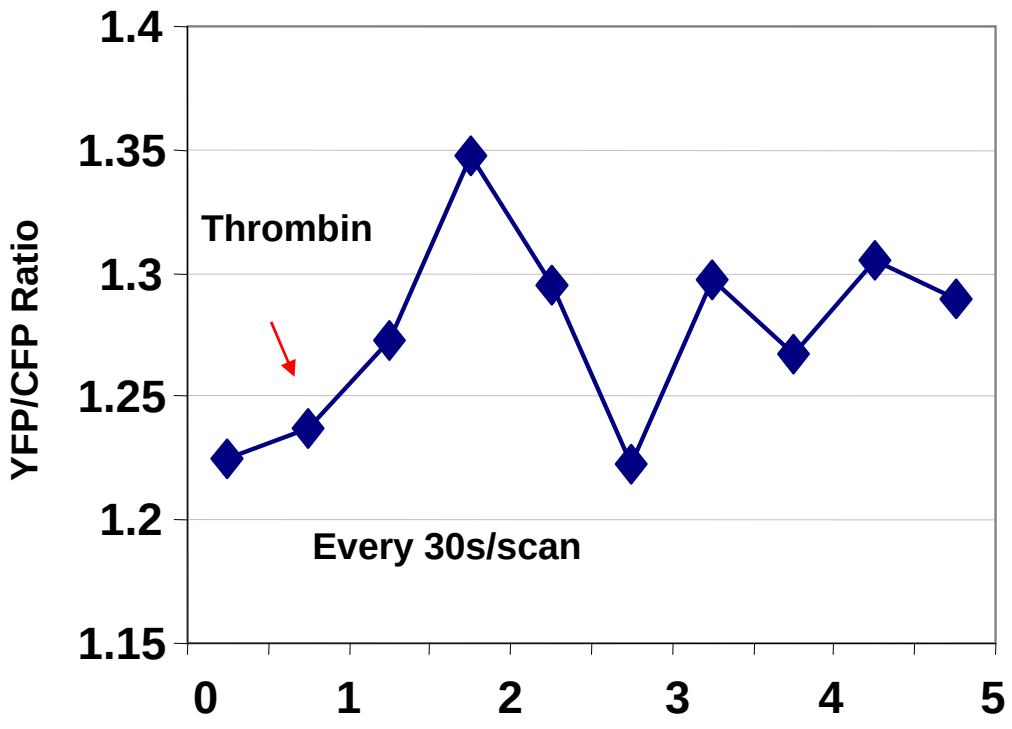

C

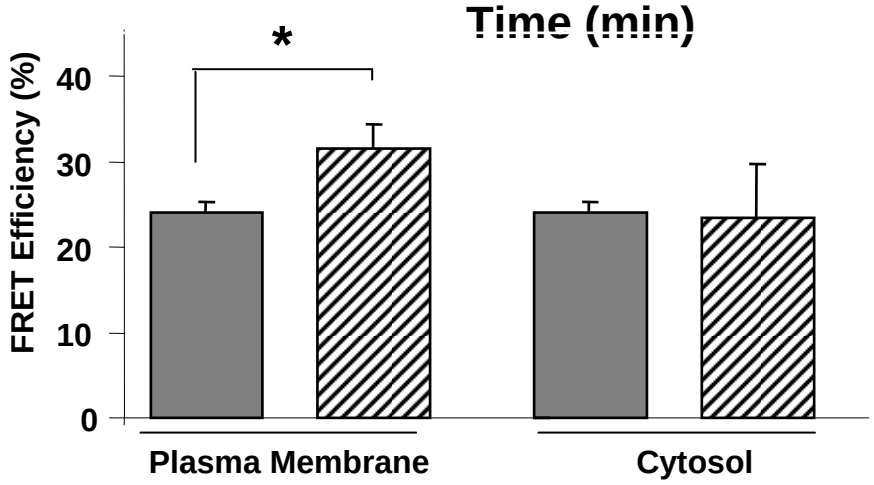

Suppl Figure II

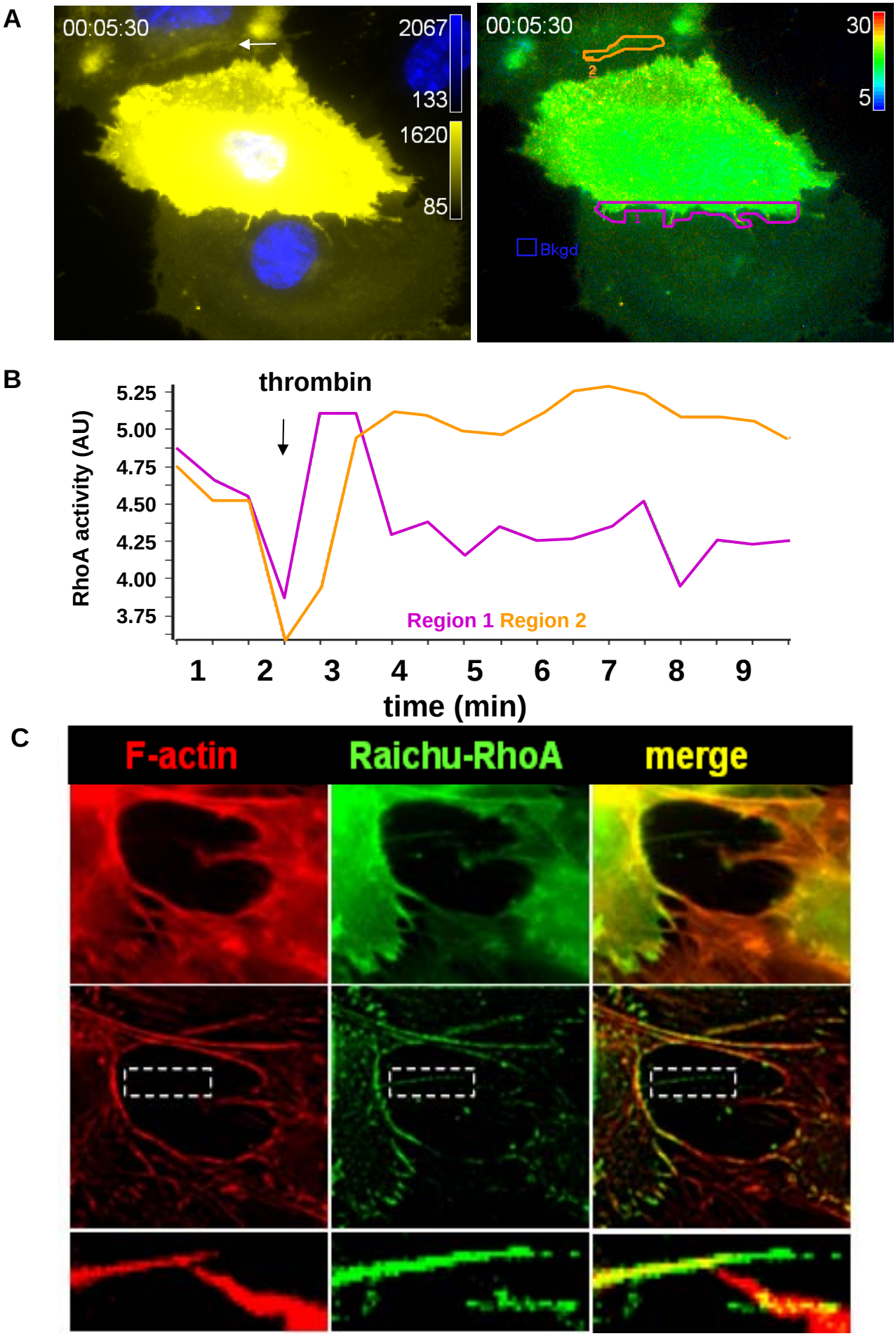

Suppl Figure III

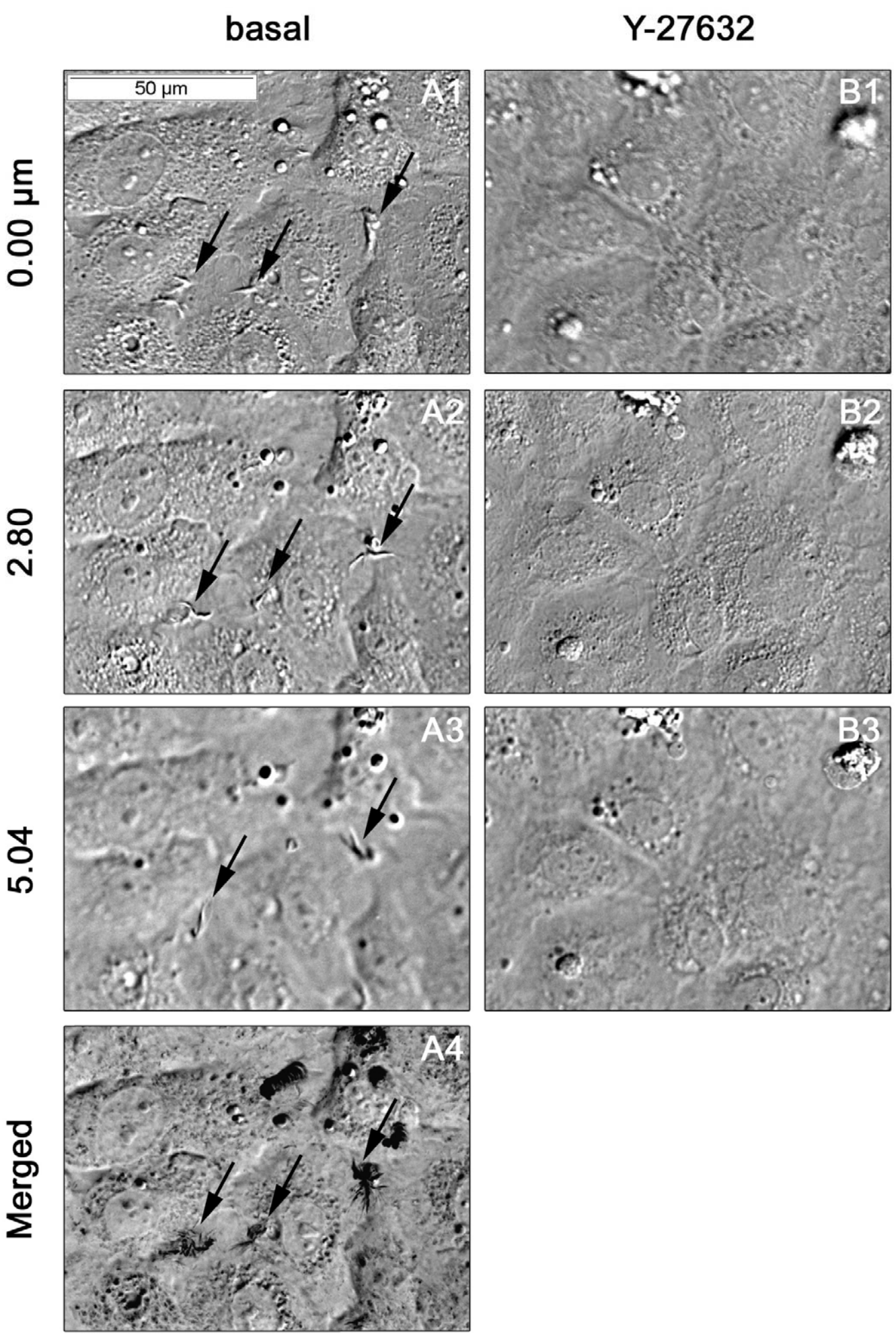

Suppl Figure IV

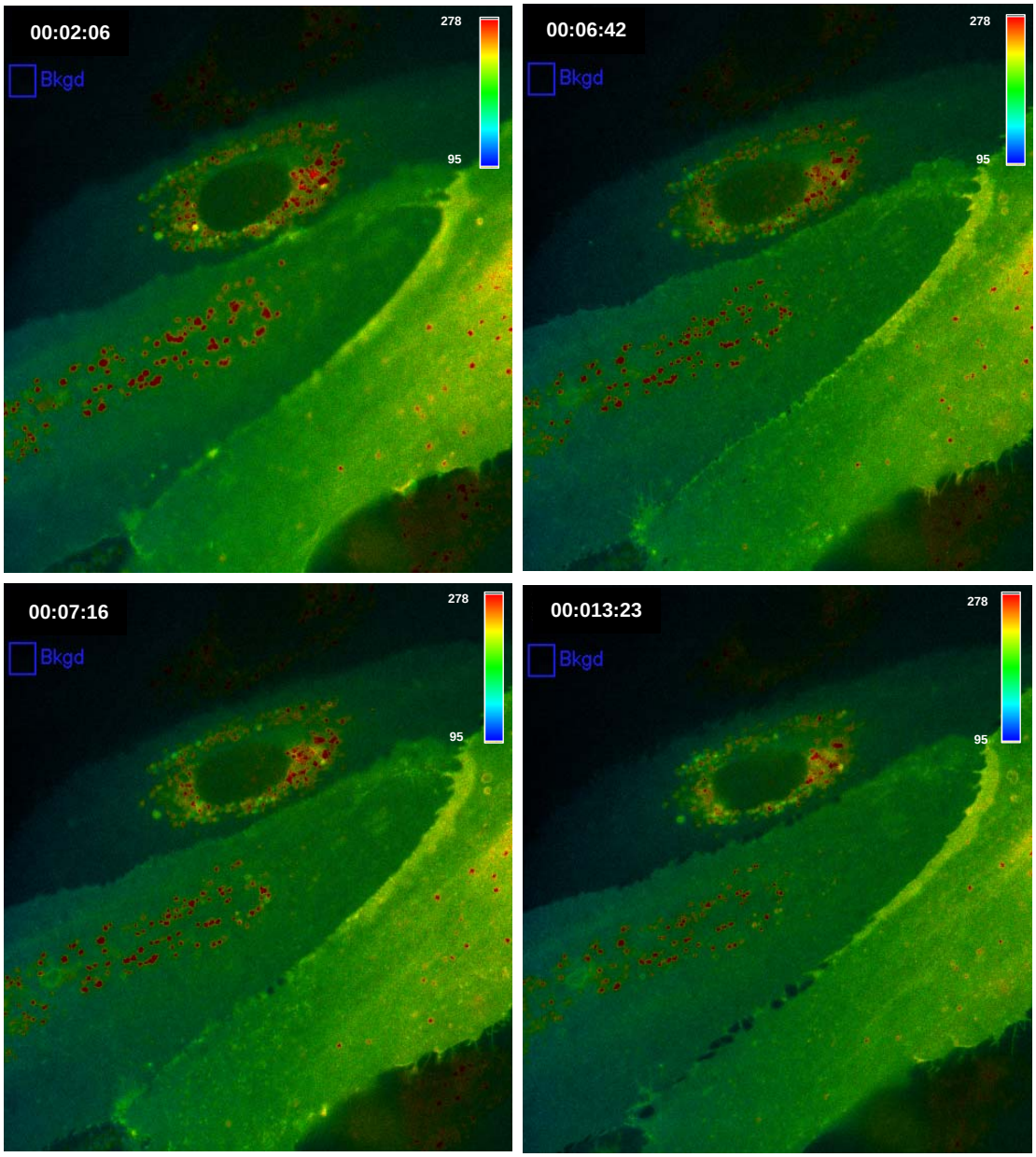

Supplemental Figure V: VEGF-induced inter-endothelial gap formation is not preceded by local RhoA activation.
Time-lapse imaging of Raichu-RhoA transfected HUVECs grown on Delta T dishes. ECs were stimulated with VEGF (25 ng/ml) at t=2.5 min.

Suppl Figure V